Journal of Alloys and Compounds 585 (2014) 529–534

Contents lists available at ScienceDirect

Journal of Alloys and Compounds

journal homepage: www.elsevier.com/locate/jalcom

An *ab initio* molecular dynamics study on the structural and electronic properties of AlB_2, TiB_2 and $(Al_x,Ti_{(1-x)})B_2$ in Al–Ti–B master alloys

H.L. Zhang, Y.F. Han *, J. Wang, Y.B. Dai, B.D. Sun *

State Key Laboratory of Metal Matrix Composites, Shanghai Jiao Tong University, 800 Dongchuan Road, Shanghai 200240, PR China

ARTICLE INFO

Article history:
Received 22 July 2013
Received in revised form 9 September 2013
Accepted 26 September 2013
Available online 8 October 2013

Keywords:
Diborides
Electronic structure
Ab initio molecular dynamics simulation
Grain refinement
Aluminum

ABSTRACT

The structural and electronic properties of AlB_2, TiB_2 and $(Al_x,Ti_{(1-x)})B_2$ diborides in Al–Ti–B master alloys are investigated by *ab initio* molecular dynamics calculations at high temperature. It is found that the dominant bonding states of AlB_2 and TiB_2 at 1073 K are ionic and covalent, respectively. The larger linear thermal expansion coefficient of AlB_2 than that of TiB_2 results from their different bonding nature. The original ionic or covalent bonding states of Al or Ti with B atoms is reversed to be covalent or ionic to suit the whole bonding environment of the diborides when Al or Ti atoms acts as the solute atoms replacing Ti or Al atoms to form $(Al_x,Ti_{(1-x)})B_2$ duplex diborides. The inter-layer cohesion in $(Al_x,Ti_{(1-x)})B_2$ diborides is weakened owing to the weakened bonding and enhanced anti-bonding of Al–B and Ti–B bonds. The thermal stability of $(Al_x,Ti_{(1-x)})B_2$ duplex diborides compared with AlB_2 and TiB_2 are elucidated from thermodynamic considerations. The higher formation energy of $(Al_x,Ti_{(1-x)})B_2$ duplex diborides is a barrier for restricting the transformation from AlB_2 to TiB_2.

1. Introduction

The Al–Ti–B master alloys are widely used in the grain refinement of aluminum and its alloy in industry, since several grain refining particles in the master alloys, such as AlB_2, TiB_2 and $TiAl_3$, are proved to be effective substrates to induce the heterogeneous nucleation of aluminum alloys [1]. For example, during the grain refinement of 1××× Al alloys, TiB_2 particles released from the Al–5Ti–1B master alloy are believed to serve as main substrates for the heterogeneous nucleation of α-Al [2]. Whereas the dominating heterogeneous nucleation sites responsible for grain refinement of Al–Si alloys are regarded as AlB_2 rather than TiB_2, and Al–1Ti–3B and Al–3B master alloys instead of Al–5Ti–1B are employed as the refiner for these alloys due to a higher efficiency of releasing AlB_2 [3].

The Al–Ti–B master alloys are usually prepared through adding a mixture of K_2TiF_6 and KBF_4 into Al melts in industry, and the contents of different components are controlled by the atom ratio and the preparation time. In the preparation of the Al–5Ti–1B master alloy, the reaction time is usually controlled longer than 60 min to guarantee a sufficient TiB_2 to help the following grain refinement in pure aluminum [4]. However, the transformation from AlB_2 and TiB_2 is still is under dispute. Since AlB_2 and TiB_2 is isomorphous, some believed that prolonged holding time after the completion of the reaction during the preparation resulted in the formation of $(Al_x,Ti_{(1-x)})B_2$ duplex diborides, which might have better potency to nucleate aluminum than aluminide and diboride particles [5]. Some observations [6,7] of the duplex particles in the experiments were reported, and Kiusalaas [8] proposed that a transformation from $(Al_x,Ti_{(1-x)})B_2$ to TiB_2 occurred during holding the preparation in the solid as well as in the liquid phase. Besides, Sigworth [9] considered that these duplex diborides were stable phase based on thermodynamic calculations. However, there are some controversies on the existence of the duplex $(Al_x,Ti_{(1-x)})B_2$ diborides. Guzowaski et al. [10] have pointed out that duplex diborides are nothing other than mixtures with boride crystals entrapped in aluminide particles. Zupanič et al. [11,12] reported that TiB_2 and AlB_2 coexist even after 1000 h exposure at 1073 K, and the formation of mixed diborides $(Al_x,Ti_{(1-x)})B_2$ were never observed, but only apparently pure AlB_2 and TiB_2 were present. They considered that the mixed diboride $(Al_x,Ti_{(1-x)})B_2$ was not a thermodynamically stable phase in the aluminum rich corner of the Al–Ti–B system.

Due to the same graphite-like structure and similar lattice parameters between AlB_2 and TiB_2 (the difference is less than 1% [13]), it is difficult to distinguish these diborides through conventional X-ray diffraction (XRD) analysis [14]. These diboride particles are imbedded in the Al matrix of master alloys, and therefore the α-Al coating these diborides could induce great errors on their Al composition by the energy dispersive spectrometer (EDS) analysis. Accordingly, it is experimentally hard to reveal the properties difference between AlB_2 and TiB_2 in the Al–Ti–B master alloys [11]. Instead, some theoretical calculations have been

* Corresponding authors. Tel.: +86 21 5474 2661; fax: +86 21 5474 5387.
E-mail addresses: yfhan@sjtu.edu.cn (Y.F. Han), bdsun@sjtu.edu.cn (B.D. Sun).

0925-8388/$ - see front matter © 2013 Elsevier B.V. All rights reserved.
http://dx.doi.org/10.1016/j.jallcom.2013.09.179

carried out to study the electronic structures of AlB_2 and TiB_2 [15–23]. For example, Oguchi considered that the AlB_2 has the strongest bonding in AlB_2-type diborides by calculating on their heat of formation [18]. Tian et al. found that the TiB_2 has the highest stability among all transition-metal diborides [20]. However, a majority of these reports, including the former work in our group [21,22], only investigated the ground state of these diborides at 0 K, which may not coincide with the real experiment and industrial preparation process at high temperature. Moreover, the properties of uncertain $(Al_x,Ti_{(1-x)})B_2$ particles including the structural and the electronic properties have never been under investigation by theoretical calculations.

In this paper, the properties of AlB_2, TiB_2 and uncertain $(Al_x,Ti_{(1-x)})B_2$ duplex diborides in Al–Ti–B master alloys were calculated at high temperature using *ab initio* molecular dynamics (AIMD) method. It is expected to reveal the electronic properties of these diborides, which could make a contribution to the further study on heterogeneous nucleation in Al melts with these diborides, and to provide evidences at atomic scale to clarify the dispute on stability of $(Al_x,Ti_{(1-x)})B_2$ diboride in Al–Ti–B master alloys.

2. Computational methodology

All the calculations were performed by first-principles method with the exchange–correlation functions as parameterized by Perdew, Burke, Ernzerhof (PBE) version [24] of the generalized gradient approximation (GGA), with the plane-wave cutoff energy of 380 eV. The ultrasoft pseudo-potentials of Vanderbilt [25] were employed for all the B, Al and Ti atoms, which define the atom configuration of B, Al and Ti are $2s^22p^1$, $3s^23p^1$, and $3s^23p^63d^24s^2$, respectively. A self-consistent field (SCF) tolerance of 1×10^{-6} eV/atom was used for all the SCF iterations. For all the molecular dynamical (MD) calculations, the time step was employed as 0.5 fs, which can ensure a convergence that the fluctuation in Hamiltonian was less than 0.1‰. We ran all the MD simulations for $2.5 \sim 3$ ps to guarantee the final equilibrium.

The simulated temperature was employed as 1073 K, which is not only the common preparation temperature of Al–Ti–B master alloys in industry, but also the reaction temperature for the hypothetical transformation from $(Al_x,Ti_{(1-x)})B_2$ to TiB_2. To obtain the initial structural and electronic configuration of these diborides, the lattice parameters and density of states (DOS) of AlB_2 and TiB_2 at the ground state were firstly calculated through AIMD at 0 K. The calculated initial lattice parameters of AlB_2 and TiB_2 were $a = 3.003$ Å, $c = 3.293$ Å for AlB_2 and $a = 3.029$ Å, $c = 3.220$ Å for TiB_2, respectively, which are quite similar with other calculated and experimental results [23,26]. Then, we built the initial configurations of continuous series of $(Al_x,Ti_{(1-x)})B_2$ duplex particles by gradually substituting one Ti atom for one Al atom in the AlB_2 supercell optimized at 0 K. It is assumed that all the substitutions were located in one Al layer of AlB_2 cell and hence five $(Al_x,Ti_{(1-x)})B_2$ duplex diborides with different substitution ratios, $(Al_{(1/6)},Ti_{(5/6)})B_2$, $(Al_{(1/3)},Ti_{(2/3)})B_2$, $(Al_{(1/2)},Ti_{(1/2)})B_2$, $(Al_{(2/3)},Ti_{(1/3)})B_2$ and $(Al_{(5/6)},Ti_{(1/6)})B_2$, were obtained. Subsequently, these duplex models were secondly optimized in NPT ensemble at 1073 K to reach their own balanced cells. Finally, we calculated the density of state (DOS) and electron populations of these diboride based on the final equilibrium at 1073 K. To precisely provide a direct evidence on the electronic structures of these diborides, all the calculations related to the electronic properties were performed with a dense $7 \times 7 \times 8$ k-mesh.

3. Results and discussion

3.1. Structural and electronic properties of AlB_2 and TiB_2

The calculated lattice parameters of AlB_2 and TiB_2 at different temperatures are shown in Fig. 1. It is seen that the TiB_2 and AlB_2 lattices are linearly expanded with increasing the temperature from 273 K to 1073 K. The balanced parameters at 1073 K and average linear thermal expansion coefficients of TiB_2 and AlB_2 from 273 K to 1073 K calculated by the slopes of fitted lines are listed in Table 1. According to the average linear thermal expansion coefficients of TiB_2, the extrapolated lattice parameters of TiB_2 at 1273 K would be $a = 3.0599$ Å and $c = 3.2620$ Å, which coincides with the early report ($a = 3.060$ Å, $c = 3.260$ Å) [16]. The accuracy of our simulation at high temperature is believable. It is noticed that the thermal expansions of parameters a and c of AlB_2 are both larger

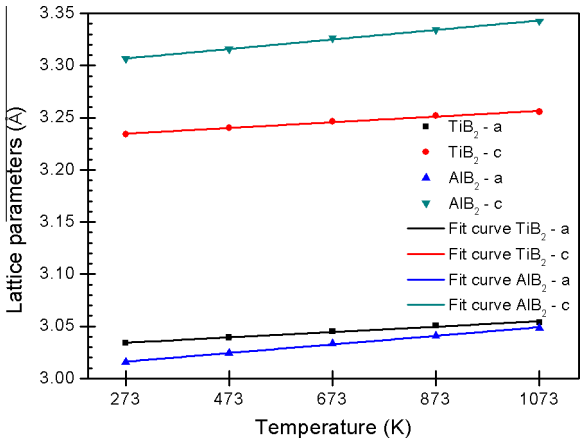

Fig. 1. The calculated lattice parameters of AlB_2 and TiB_2 at different temperatures and their linear fitting with increasing temperature.

than those of TiB_2. The larger linear thermal expansion coefficient of AlB_2 indicates a weaker cohesion than that in TiB_2 at high temperatures. Despite the thermal expansion, c/a ratios for both AlB_2 and TiB_2 nearly remain constant, which are 1.096 for AlB_2 and 1.066 for TiB_2, respectively, indicating good thermal stabilities of both AlB_2 and TiB_2.

The different structural properties of TiB_2 and AlB_2 at high temperature could be elucidated through their electronic properties. Their total and partial density of states (DOS and PDOS) around Fermi energy at 1073 K are shown in Figs. 2 and 3, respectively. For TiB_2, the 3*s* and 3*p* states of titanium, which are mainly localized far below the Fermi energy, have little impact on the bonding and cohesion of these diborides. The total bonding states of TiB_2 near the Fermi energy are mainly composed of 3*d* and 4*s* states of titanium and 2*s* and 2*p* states of boron. The PDOS of boron in TiB_2 (Fig. 2(c)) describes a total overlap between 2*s* and 2*p* states in the whole range. The PDOS of titanium shows two high peaks of 3*d* states and residual *s* and *p* states around Fermi energy, and both the *s* and *p* states overlap with the 3*d* states in the whole range. The residual *s* and *p* states around Fermi energy result from the hybridization among Ti 3*d*, 4*s* and 4*p* states, because the admixed 4*p* states with the entire valence band of Ti could interact with Ti 3*d* and 4*s* states as stated in earlier reports [27,28]. The Ti-3*d* states draw a strong hybridization with B-2*p* states, which contributes to the steep pseudogap at Fermi energy in the total DOS of TiB_2. Accordingly, we could draw clear conclusions on the electronic properties of TiB_2 at 1073 K. The localized 3*s* and 3*p* states of titanium in TiB_2 do not involve into the bonding states and contribute little to the cohesion of TiB_2. The overlap between the B-2*s* and B-2*p* states results in the sp^2 hybridization, which forms the 2D hexagonal boron network as the dominant inner-layer cohesion in the boron layer. Whereas the weak metallic bonding resulting from the hybridization among Ti-3*d*, Ti-4*s* and Ti-4*p* forms the main inner-layer cohesion of the titanium layer. On the other hand, the *d*-*p* hybridization between Ti-3*d* and B-2*p* states serves as the major inter-layer cohesion of TiB_2. The Ti–B covalent interactions can lower the energy of the bonding states and increase the energy of anti-bonding states, which produces the pseudogap at Fermi level [20]. Therefore, covalent bonding is the dominant cohesion of TiB_2, which leads to its great structural stability at high temperature.

Compared with TiB_2, the total DOS of AlB_2 contains less bonding states and draws more "smoothly" (Fig. 3(a)). The overlap between B-2*s* and B-2*p* states (Fig. 3(c)) also indicates the sp^2 hybridization. However, the energy range of the hybridization is wider and the anti-bonding states above the Fermi energy are